Published in final edited form as:

Sci Signal. ; 10(467): . doi:10.1126/scisignal.aah4674.

Pentraxin-3 is a PI3K signaling target that promotes stem cell–like traits in basal-like breast cancers

Clémence Thomas[1], **Whitney Henry**[1], **Benjamin G. Cuiffo**[1], **Anthony Y. Collmann**[1], **Elisabetta Marangoni**[2], **Vanessa Benhamo**[2], **Manoj K. Bhasin**[3], **Cheng Fan**[4], **Laetitia Fuhrmann**[2], **Albert S. Baldwin**[4], **Charles Perou**[4], **Anne Vincent-Salomon**[2], **Alex Toker**[1], and **Antoine E. Karnoub**[1,5,6,*]

[1]Department of Pathology and Cancer Center, Beth Israel Deaconess Medical Center, Harvard Medical School, Boston, MA 02215, USA

[2]Institut Curie, Paris Cedex 05, France

[3]Department of Medicine, Beth Israel Deaconess Medical Center, Harvard Medical School, Boston, MA 02215, USA

[4]Lineberger Comprehensive Cancer Center, University of North Carolina at Chapel Hill, Chapel Hill, NC 27599, USA

[5]Harvard Stem Cell Institute, Cambridge, MA 02138, USA

[6]Broad Institute of Massachusetts Institute of Technology and Harvard, Cambridge, MA 02142, USA

Abstract

Basal-like breast cancers (BLBCs) exhibit hyperactivation of the phosphoinositide 3-kinase (PI3K) signaling pathway because of the frequent mutational activation of the *PIK3CA* catalytic subunit and the genetic loss of its negative regulators PTEN (phosphatase and tensin homolog) and INPP4B (inositol polyphosphate-4-phosphatase type II). However, PI3K inhibitors have had limited clinical efficacy in BLBC management because of compensatory amplification of PI3K downstream signaling loops. Therefore, identification of critical PI3K mediators is paramount to

*Corresponding author. akarnoub@bidmc.harvard.edu.

SUPPLEMENTARY MATERIALS

www.sciencesignaling.org/cgi/content/full/10/467/eaah4674/DC1

Fig. S1. Gene set enrichment analysis of activated PIK3CA–regulated genes in MCF10A basal-like breast cells.

Fig. S2. PTX3 is regulated by NF-κB–dependent pathways.

Fig. S3. PTX3 triggers CSC-like traits.

Data file S1. PTX3 expression across multiple cell lines in the Broad Institute CCLE.

Author contributions: C.T., W.H., B.G.C., A.Y.C., E.M., V.B., M.K.B., C.F., L.F., and A.E.K. collected the data and performed the analyses. A.S.B., C.P., A.V.-S., A.T., and A.E.K. supervised the research. A.E.K. designed the study and wrote the manuscript, with input from the co-authors.

Competing interests: C.P. is a paid consultant for Biomodels LLC, is an equity stock holder and member of the Board of Directors for Bioclassifier LLC, and is listed as an inventor on patent applications for the breast PAM50 assay. The other authors declare that they have no competing interests.

Data and materials availability: Gene expression data have been deposited to Gene Expression Omnibus under accession no. GSE93422. Requests for plasmids and other reagents need to be made to A.E.K.

the development of effective BLBC therapeutics. Using transcriptomic analysis of activated PIK3CA–expressing BLBC cells, we identified the gene encoding the humoral pattern recognition molecule pentraxin-3 (PTX3) as a critical target of oncogenic PI3K signaling. We found that PTX3 abundance is stimulated, in part, through AKT- and nuclear factor κB (NF-κB)–dependent pathways and that presence of PTX3 is necessary for PI3K-induced stem cell–like traits. We further showed that *PTX3* expression is greater in tumor samples from patients with BLBC and that it is prognostic of poor patient survival. Our results thus reveal PTX3 as a newly identified PI3K-regulated biomarker and a potential therapeutic target in BLBC.

INTRODUCTION

Basal-like breast cancer (BLBC) comprises a heterogeneous group of tumors that collectively account for ~15% of all breast cancers (1). They are more common in younger women, particularly of African-American descent (2, 3), and typically present with undifferentiated triple-negative breast cancer (TNBC) histological features and aggressive clinical behavior (4–6). BLBCs are, in their majority, unresponsive to current treatment regimens (7, 8), and refractory patients experience dismal outcomes with increased rates of recurrence within 1 to 3 years and heightened mortality rates within 5 years (5). Effective and targeted therapeutic approaches for BLBCs are therefore critically needed but remain to be defined.

At the molecular level, BLBCs display marked deregulations in a number of tumor suppressor pathways, such as p53, pRb, and BRCA1 (1). They also exhibit prominent activation of phosphoinositide 3-kinase (PI3K)–AKT signaling, a phenotype that is due, in part, to frequent loss of the PI3K pathway antagonists phosphatase and tensin homolog (PTEN) and inositol polyphosphate-4-phosphatase type II (INPP4B) (9). However, antagonizing PI3K activity in the context of BLBC clinical management is hampered by the emergence of resistance to a variety of PI3K inhibitors (10). Such resistance mechanisms do not seem to originate from the acquisition of secondary mutations in PI3K but, rather, by a series of compensatory mechanisms that amplify signal transduction pathways downstream of PI3K (11, 12). Therefore, identifying and inhibiting critical mediators of PI3K oncogenic activity would aid in the development of new and effective therapies targeting BLBC.

Here, we set out to identify previously unknown downstream effectors of PI3K in BLBC cells by conducting differential whole-genome transcriptomic analyses of basal-like MCF10A cells expressing an activated mutant of the catalytic subunit of PI3K ($PIK3CA^{H1047R}$), a recurrent and frequent mutation observed in all molecular subtypes of breast cancer. We identified the inflammatory protein pentraxin-3 (PTX3) as a mediator of PI3K signaling and found that its presence is both necessary and sufficient for the acquisition of stem cell–like growth traits in BLBC cells. Our results revealed new functions for PTX3 as a PI3K-regulated biomarker, a supporter of stem-like phenotypes in breast cancer cells (BCCs), and a potential therapeutic target in BLBC.

RESULTS

PI3K activation induces *PTX3* expression in BLBC cells through AKT- and nuclear factor κB–dependent signaling

Comparative gene expression–based analysis of PIK3CA^{H1047R} and wild-type (13) MCF10A cells revealed a significant [>1.5-fold; false discovery rate (FDR), 0] induction of 231 genes in PIK3CA^{H1047R}-expressing cells, which clustered into multiple gene sets using the Database for Annotation, Visualization and Integrated Discovery (DAVID) gene set enrichment analysis software (fig. S1A) (14). Twenty-one of the 231 induced genes belonged to the inflammatory response gene set (enrichment score, 11.13; $P = 3.4 \times 10^{-10}$), with the top hit being the inflammatory mediator PTX3, induced by PIK3CA^{H1047R} ~3.9-fold compared to wild-type cells (Fig. 1A and fig. S1B). PTX3 is a member of the pattern recognition molecule family of proteins and is expressed in a variety of cell types, particularly in hematopoietic and stromal cells responding to inflammatory signals such as interleukin-1β, tumor necrosis factor–α, or Toll-like receptor agonists (15). It is an acute phase protein that exerts pleiotropic protective functions in innate immunity, which include associating with microbial moieties, binding to certain microorganisms, facilitating pathogen recognition, activating complement cascades, and exhibiting opsonic activities (16). PTX3 also exerts critical roles in the clearance of apoptotic cells, in leukocyte recruitment into inflamed tissues (17), and in matrix deposition during normal (such as oocyte cumulus) (18, 19) or pathogenic matrix remodeling, such as after tissue injury (20, 21). This evidence suggests a central role for PTX3 in regulating both local and systemic inflammation. Whether PTX3 serves any role in BLBC, however, has not been determined.

PTX3 induction by PIK3CA^{H1047R} expression was validated by RNA (Fig. 1B) and protein (Fig. 1C) determination, which revealed several-fold enrichment of each in PIK3CA^{H1047R} cells. Conversely, inhibition of PI3K signaling by the pan-PI3K inhibitor BKM120 in PIK3CA^{H1047R}-expressing MCF10A cells (Fig. 1C), by PIK3CA-specific short hairpin RNAs (shRNAs) in SUM159 cells (which harbor an endogenous H1047L-activated allele of PIK3CA) (Fig. 1D), or by the PI3K inhibitors BEZ235, BYL719, and BKM120 in SUM159 and MDA-MB-231 cells (Fig. 1, E and F) inhibited both induced and basal PTX3 abundance suggesting that the PI3K pathway is critical to PTX3 expression. Furthermore, increased *PTX3* expression correlated with PI3K pathway activation both in mouse models (Fig. 1G) and in clinical specimens (Fig. 1H). Notably, *PTX3* expression correlated negatively with that of *PTEN* and *INPP4B* in breast tumors (Fig. 1H), further indicating that PTX3 may be regulated by activated PI3K signaling in multiple contexts.

We next investigated how PI3K might regulate *PTX3* expression. Treating serum-starved SUM159 cells with MKK2206, a specific allosteric AKT inhibitor, suppressed endogenous PTX3 protein abundance (Fig. 1I), suggesting that AKT activation promotes PTX3 abundance in PIK3CA^{H1047R} -driven SUM159 cells. However, the fact that residual PTX3 remained afterMKK2206 treatment suggested that PTX3 is likely regulated by additional AKT-independent pathways as well.

AKT stimulates the phosphorylation of Ser^{176} and Ser^{180} of IKKα [inhibitor of nuclear factor κB (NF-κB) (IκB) kinase α] and Ser^{177} and Ser^{181} of IKKβ, which in turn causes the

degradation of IκB (through phosphorylation at Ser^{32} and Ser^{36}), while also activating p65 by phosphorylating it at Ser^{536} (22). In light of this connection and the fact that the proximal promoter of *PTX3* contains two strong NF-κB consensus sites (fig. S2C), we analyzed NF-κB involvement in PI3K regulation of PTX3 expression. As predicted, $PIK3CA^{H1047R}$ stimulated NF-κB activation in MCF10A cells as revealed by the phosphorylation of IKKα/β $Ser^{176/180}$, IκB $Ser^{32/36}$, and p65 Ser^{536}, along with down-regulation of total IκB abundance when compared to controls (Fig. 1J). Treatment of these cells with the IKKβ adenosine 5′-triphosphate (ATP)–competitive inhibitor compound A, which inhibits the phosphorylation of IκB and p65, almost completely diminished $PIK3CA^{H1047R}$-induced PTX3 abundance (Fig. 1J). These results were also observed in SUM159 cells, in which compound A reduced the abundance of PTX3 mRNA and protein (fig. S2, D and E). Together, these observations suggested that PTX3 is regulated in part by AKT- and NF-κB–dependent signaling pathways.

PTX3 expression is specifically associated with BLBC cells

We next explored the involvement of PTX3 in breast cancer pathogenesis by examining the expression of *PTX3* across publicly available clinical breast cancer gene expression data sets derived from the four major molecular subtypes of breast cancer: BLBC, human epidermal growth factor receptor 2 (HER2)–enriched, luminal A (LumA), and LumB. We found that *PTX3* abundance was enriched (two- to seven-fold) in BLBC when compared to HER2, LumA, or LumB subgroups in a number of studies that included GSE1561 (23), GSE1456 (24), TCGA (9), and UNC337 (Fig. 2, A to D) (25). The preponderance of *PTX3* in BLBC was also observed in our own profiled breast cancer specimens collected at the Curie Institute (Fig. 2E) and was generalized to BLBCs compared to all non-BLBCs grouped together in the Dana-Farber Cancer Institute GSE7904 cohort (Fig. 2F) (26). Together, these observations indicated that *PTX3* is particularly and abundantly expressed in BLBC.

PTX3 expression described above was derived from minced tumor tissues, which contain both cancer cells and their associated stroma. BLBCs are distinguished from other breast cancer subtypes by exhibiting high levels of immune cell infiltrates that can express PTX3 (1, 15). To investigate whether cancer cells in clinical BLBC specimens expressed *PTX3* per se, we dissected cancer cells from representative slides of the respective breast cancer subtypes and assessed *PTX3* expression in the harvested RNA using qRT-PCR. In keeping with our genomic-based observations, BLBC cancer cells exhibited multifold enrichment of *PTX3* compared to reduction mammoplasty–derived control tissues (Fig. 2G), whereas cancer cells derived from HER2, LumA, and LumB tumors displayed a 6- to 20-fold decrease in *PTX3* expression when compared to controls or BLBC cells (Fig. 2G). Similar to MCF10A cells expressing $PIK3CA^{H1047R}$, BCC lines associated with BLBC displayed, on average, >13-fold enrichment in *PTX3* mRNA when compared to non-BLBC cancer cells, such as ZR75, MCF7, SKBR, or T47D cells (Fig. 2H), underscoring the tight association between PTX3 and BLBC.

We also evaluated the extent to which these observations can be generalized to multiple different BCC lines. For this purpose, we used the Broad Institute Cancer Cell Line Encyclopedia (CCLE) to identify a “PTX3 signature” that we then used to probe cell lines of

interest. We identified 19 genes that are mostly coexpressed with PTX3 across >260 cancer cell lines in the database (data file S1). We observed that this signature was enriched in BLBC cell lines, such as HCC1143, BT549, Hs578T, and MDA-MB-436, when compared to HER2 and luminal cell lines, such as HCC1954, MDA-MB-415, or BT474, which appear to be unanimously devoid of such expression patterns (Fig. 2I). These results confirm that PTX3 and its associated signature are highly and particularly enriched in BLBC.

PTX3 promotes cancer stem cell–like traits

The tight association of the PTX3 signature with BLBC prompted us to investigate whether PTX3 is further confined into a particular BLBC subset. As BLBCs are predominantly considered TNBCs because they mostly lack estrogen receptor and progesterone receptor expression as well as ERBB2 (also known as HER2) overexpression and/or amplification (4), we examined the enrichment of PTX3 signature in the six molecular TNBC subclasses proposed by Lehmann *et al.* (27): basal-like 1 (BL1), BL2, immunomodulatory (IM), mesenchymal (M), mesenchymal stem cell–like (M/MSL), and luminal androgen receptor (LAR)–positive tumors. These analyses revealed that PTX3 and its associated genes clustered more evidently with the M/MSL cells (six of six cell lines), whereas BL1/BL2 cell lines showed moderate-to-low expression, followed by the IM and LAR counterparts, which displayed depleted expression (Fig. 3A). Immunoblot analysis of the lysates of some of the lines presented in Fig. 3A also revealed preferential expression of the PTX3 protein in the M/MSL group (three of four cell lines) when compared to BL1, BL2, and LAR cells (one of seven cell lines; Fig. 3B). Moreover, increased *PTX3* expression was observed in M/MSL patient-derived xenograft (PDX) models of breast cancer (M/MSL > BL1/2 ⋙ LAR/IM; Fig. 3C), further supporting a link between PTX3 expression and the M/MSL group.

The M and MSL subtypes are enriched for genes/pathways that regulate, among others, cellular motility, extracellular matrix interactions, and cellular differentiation and are reminiscent of the intrinsic claudin-low (CL) phenotype, as previously characterized (25). M/MSL/CL subtypes share common features that include enrichment in genes encoding the proteins that regulate epithelial-to-mesenchymal transition (EMT; such as SNAIL and TWIST), low expression of tight junction proteins (such as claudins 3, 4, and 7), and increased abundance of genes encoding proteins associated with cancer stem cells (CSCs; such as ALDHA1 and HOX). When BCC lines were aligned according to the CL classification, we noticed a robust up-regulation of the PTX3 gene signature in six of seven queried cell lines (Fig. 3D). Moreover, although PTX3 abundance was increased in cells such as Hs578T, SUM159, or MDA-MB-231, which also cluster with CL cells (25), we found detectable PTX3 abundance in HCC1143 and HCC38 cells, as well as high abundance in SUM149 cells (Fig. 3B), and BL1/2 cell lines contained significant numbers of CL cells within them (25). We further tested the association of PTX3 with the CL phenotype by probing human mammary epithelial (HMLE) cells that exogenously express the embryonic transcription factors goosecoid (GSC), SNAIL, and TWIST, variants that segregate along the CL subtype (28). Here too, *PTX3* expression was induced 5- to 15-fold (Fig. 3E). Finally, CL clinical samples extracted from UNC337 exhibited comparable enrichment in *PTX3* versus their BLBC counterparts (Fig. 3F). Together, these findings support a strong association between PTX3 and the M, MSL, and CL breast cancer subtypes.

As discussed above, the M, MSL, and CL subtypes are characterized by overrepresentation of genes associated with EMT and CSC regulation, and M/MSL/CL tumors have such features (25, 27). In addition, the PTX3-associated gene expression signature revealed genes implicated in stem cell and/or EMT state regulation in BLBC, such as *LOX* (29), *LOXL2* (30), *COL6A1/2* (31), *AXL* (32), *VEGFC* (33), and *SPARC* (34). We therefore evaluated whether PTX3 regulated EMT or CSC traits in basal-like mammary epithelial cells. We found that stable over-expression of PTX3 from a pBabe retroviral construct in MCF10A cells did not cause significant down-regulation of epithelial markers (such as zonula occludens-1 or E-cadherin) (fig. S3A), did not promote up-regulation of mesenchymal markers (such as fibronectin, smooth muscle actin, or vimentin) (fig. S3B), and did not cause any detectable morphological changes in the cells relative to control counterparts (fig. S3C), indicating that PTX3 alone is not sufficient in triggering EMT in these contexts. In contrast, PTX3-overexpressing MCF10A cells were able to form twice as many tumorspheres in suspension compared to control cells (Fig. 4A), exhibited significant enrichment (16%) in their $CD44^{hi}/CD24^{low/neg}$ CSC-like populations (Fig. 4B), and displayed a fourfold increase in their positivity for the CSC-associated marker aldehyde dehydrogenase 1 (ALDH1) (Fig. 4C) (35). Similar observations were made in MDA-MB-231 and BT549 cells, where ectopic PTX3 expression enhanced primary and secondary tumorsphere formation and ALDH1 positivity (fig. S3, D and E). Furthermore, we found that inhibiting the expression of endogenous PTX3 in SUM159 cells using shRNAs (shPTX3) caused up to 40% inhibition in $CD44^{hi}/CD24^{low/neg}$ (Fig. 4D) and almost abrogated ALDH1 positivity in SUM159 and MDA-MB-231 cells (Fig. 4D and fig. S3F). These observations suggested that PTX3 is involved in regulating CSC-like phenotypes in basal-like breast cells.

To assess the functional contributions of PTX3 to PI3K signaling, we inhibited PTX3 expression using shRNAs in the background of PI3K activation. We and others have previously shown that PI3K signaling mediates cell proliferation under growth factor deprivation and that it strongly regulates stem cell traits in breast (and other) cancer cells (36–38). $PIK3CA^{H1047R}$ promoted a sevenfold increase in the number of ALDH1-positive cells (Fig. 4E), stimulated cell proliferation under EGF deprivation (Fig. 4F), and mediated tumorsphere growth (Fig. 4G). Conversely, shPTX3 inhibited all these phenotypes, abrogating $PIK3CA^{H1047R}$-induced ALDH1 stimulation and inhibiting cancer cell growth in two- and three-dimensional culture assays (Fig. 4, E to G). Notably, PTX3 was a powerful prognostic indicator for worse overall survival (Fig. 4H) and worse relapse-free survival (Fg. 4I) in the UNC337 cohort, which is enriched with M/MSL/CL specimens. Collectively, our results suggest a model in which PTX3 serves as an intrinsic mediator of PI3K-regulated CSC-like traits in BLBC cells.

DISCUSSION

When compared to other breast cancer subtypes, BLBCs exhibit the highest activation patterns in the PI3K/AKT pathway (9). This is due, in part, to the frequent loss of *PTEN* and *INPP4B*, as well as to a substantial frequency of activating mutations in *PIK3CA*. Therefore, identifying signaling effectors that are critical for PI3K/AKT functions in BLBC will provide important and relevant targets for BLBC therapy. On the basis of our findings, we

propose that PTX3 represents one such signaling effector. PI3K pathway activation induced PTX3 in cellular and mouse models of BLBC and positively associated with *PTX3* expression in clinical settings. Furthermore, inhibition of PTX3 alone was sufficient to suppress PI3K-stimulated growth, strongly underscoring its functions as a critical mediator of oncogenic PI3K signaling. In support of this hypothesis are the observations that NF-κB was necessary to drive PTX3 expression and that PTX3, in turn, regulated the propagation of stem cell–like traits in cancer cells, phenotypes that are highly enriched in BLBC (39) and promoted by PI3K and NF-κB (38, 40–42). On the basis of these results, as well as the recognized role of CSC-like populations in driving BLBC malignancy (43), we speculate that PTX3 represents both a novel biomarker and a potential therapeutic target in BLBC.

How PTX3 regulates BCC growth and how it propagates CSC-like traits in BLBC cells remain to be determined. We found that PTX3 expressed by BLBC cells was soluble (fig. S3A), and therefore, it is possible that BCC-derived PTX3 acts in an autocrine/paracrine manner through its proper and yet-to-be-identified receptor(s) on the surface of cancer cells. In light of its reported activities as a rudimentary antibody (21), it is also plausible that PTX3 acts by cross-linking growth factor receptors residing at cell surfaces.

Correlative biomarker studies previously described increased in situ and/or systemic PTX3 abundance in patients with lung (44, 45), prostate (46), ovarian (13), liver (47), and pancreatic (48) tumors, as well as in those with cancer-prone myeloproliferative diseases (49), suggesting that PTX3 serves as a cancer biomarker and potentially functions in cancer-supportive roles similar to the ones described here. In breast cancer, Scimeca *et al.* (50) also correlated increased immunohistochemical PTX3 staining with poorly differentiated aggressive breast cancers and related stromal PTX3 production to increased chemotherapy resistance of BCCs (51). Although these collective findings are in support of the promalignant roles we describe for PTX3 in the present work, these observations are in sharp contrast to other studies in which PTX3 was found to exert suppressive roles in tumor pathogenesis.

However, the prevalent model for PTX3 involvement in tumor development depicts its paracrine activities as a microenvironmental factor that promotes tumor suppression. In this scheme, PTX3 was found to bind certain members of the fibroblast growth factor (FGF) family (in particular FGF2 and FGF8b), suppressing FGF-induced neovascularization and hampering tumor formation in xenograft models (52, 53). Similarly, PTX3 was shown to exert antimetastatic effects in melanoma (54) and to act as an extrinsic factor that inhibits cancer growth in a variety of additional heterotypic, syngeneic, and autochthonous prostate, lung, and pancreatic tumor models (55). These notions were further reinforced by Bonavita *et al.* (56), who showed that PTX3 ablation sensitized animals to carcinogen-induced tumorigenesis through the creation of a favorable immune tumor microenvironment that in turn stimulated oxidative stress and genetic instability in the cancer cells. These results underscore a role for PTX3 as a determining regulator of cancer-related inflammation (CRI), which exerts extrinsic activities in suppressing tumor initiation and development. Notably, the *PTX3* gene was found to be highly methylated in human tumor cells, such as in esophageal cancers (57), leiomyosarcomas (56), and colorectal cancers (56, 58), suggesting a beneficial role for certain cancer cells to suppress their intrinsic production of PTX3. In

contrast, however, our results show that *PTX3* is highly expressed in BLBC cells and that it acts as an intrinsic oncopromoter that is prognostic of worse survival outcomes in BLBCs (Fig. 1H), subtypes characterized by increased CRI (59) and heightened genetic instability (60). Collectively, our results support a model in which functions of PTX3 in cancer pathogenesis are likely to be context-dependent and that PTX3-targeting therapies need to be rationalized together with the type, genetic background, and composition of both cancer cells and their associated stroma.

MATERIALS AND METHODS

Gene expression analyses

Gene expression analysis of MCF10A cells stably expressing PIK3CA^{H1047R} versus wild-type PIK3CA were performed using a Human SurePrint G3 GE v2 platform (Agilent) as standard. Data were analyzed from triplicate runs and stratified with respect to statistical significance. Gene ontology was performed using the DAVID software (david-d.ncifcrf.gov) (14). Data are deposited in Gene Expression Omnibus (GSE93422).

Constructs

Human *PTX3* amplified from human complementary DNA of normal prostatic tissues and verified by sequencing to be free of mutations was cloned into the pBabe-puromycin plasmid obtained from R. Weinberg. Expression constructs coding for wild-type and H1047R-mutant PIK3CA, pLP-LNCX-PIK3CA-WT (Addgene plasmid #25633), and pLP-LNCX-PIK3CA-H1047R (Addgene plasmid #25635) were obtained from T. Waldman. shRNA constructs in the pLKO.1-puromycin lentiviral system raised against human *PTX3* were purchased from the RNAi Facility at the Dana-Farber Cancer Institute. For shRNAs against *PIK3CA*, single-stranded sense and antisense oligonucleotide pairs PIK3CA shRNA#1 (sense, 5′-CCGGGCACAATCCATGAACAGCATTCTCGAGAATGCTGTTCATGGATTGTGCTTTTTTG-3′), PIK3CA shRNA#1 (antisense, 5′-AATTCAAAAACACAATCCATGAACAGCATTCTCGAGAATGCTGTTCATGGATTGTG-3′), PIK3CA shRNA#2 (sense, 5′-CCGGGCATTAGAATTTACAGCAAGACTCGAGTCTTGCTGTAAATTCTAATGCTTTTTTG-3′), and PIK3CA shRNA#2 (antisense, 5′-AATTCAAAAAGCATTAGAATTTACAGCAAGACTCGAGTCTTGCTGTAAATTCTAATGC-3′) were synthesized and cloned into pLKO.1 vector. Lentiviral supernatants were collected after 48 hours from 293T cells cotransfected with the respective pLKO-shRNA constructs, VSVG and psPAX2, and used to infect target cells in the presence of polybrene. Cells stably expressing the respective shRNAs were selected and cultured in growth medium containing puromycin (2 μg/ml).

BCC lines

BCC lines MDA-MB-468, HCC1937, HCC1143, SUM149, BT549, Hs578T, SUM159, MDA-MB-231, HCC70, HCC38, ZR75, MCF7, SKBR, and T47D were purchased from the American Type Culture Collection (ATCC) and propagated according to the conditions specified by ATCC. MCF10A cells were obtained from J. Brugge (Harvard Medical School)

and were cultured in Dulbecco's modified Eagle's medium/Ham's F12 medium supplemented with 5% equine serum (Gibco BRL), insulin (10 μg/ml), hydrocortisone (500 ng/ml) (Sigma-Aldrich), EGF (20 ng/ml) (R&D Systems), and cholera toxin (100 ng/ml) (List Biological Laboratories). HMLE cells expressing GSC, SNAIL, and TWIST were obtained from R. Weinberg.

Pathway inhibitors

Inhibitors BKM120 (#A-1108), BEZ235 (#A-1009), BYL719 (#A-1214), and MKK2206 (#A-1206) were purchased from Active Biochem Co. The IKKβ ATP–competitive inhibitor compound A (61) was manufactured by Bayer Pharmaceuticals.

Western blot analyses

Cell lysates were prepared using radioimmunoprecipitation assay buffer in the presence of protease and phosphatase inhibitors, and cleared proteins were resolved by gel electrophoresis, transferred by electrophoresis to nitrocellulose membranes, and processed for Western blotting as is standard using the following antibodies: antibody against PTX3 was purchased from LSBio (#LS-C138995); antibodies against p110α (#4249), phosphorylated (phospho)–AKT Ser^{473} (#4060), phospho-AKT Thr^{308} (#2965), AKT (#4691), phospho-PRAS40 Thr^{246} (#2997), PRAS40 (#2691), phospho-GSK3β Ser^{9} (#9336), GSK3β (#9315S), phospho-p70S6K (#9204), S6P (91B2; #4857), Z0-1 (#5406 and #5406), E-cadherin (4A2, #14472), β-tubulin (#2128), N-cadherin (#4061), vimentin (#5741), p85 (#4292), β-actin (#4970), IKKα/β $Ser^{176/180}$ (#2697), phospho-IκBα $Ser^{32/36}$ (#9246), IκBα (#9247), phospho–NF-κBp65 Ser^{536} (#3033), and NF-κB p65 (#8242) were purchased from Cell Signaling Technology. Antibodies raised against fibronectin and smooth muscle actin were purchased from BD Transduction (#610078) and Abcam (ab5694), respectively. Blots were developed using horseradish peroxidase–conjugated secondary antibodies using chemoluminescence (Millipore and Chemicon).

qRT-PCR analysis

PTX3 mRNA expression was determined by qRT-PCR on total cellular RNA extracted using the RNeasy protocol (Qiagen). RNA was reverse-transcribed using QuantiTect Reverse Transcription Kit (Qiagen), and the product was amplified using SYBR Green PCR Master Mix (Bio-Rad) in an ABI Prism 7900 sequence detector (Applied Biosystems). *PTX3* mRNA abundance was determined using the $\Delta\Delta C_t$ method and normalized to GAPDH or 18*S*. Primers used were as follows: PTX3 forward, 5′-GCTCTCTGGTCTGCAGTGTT-3′ or 5′-CATCCAGTGAGACCAATGAG-3′; PTX3 reverse, 5′-CTTGTCCCATTCCGAGTGCT-3′ or 5′-GTAGCCGCCAGTTCACCATT-3′; 18*S* forward, 5′-GTAACCCGTTGAACCCCATT-3′; 18*S* reverse, 5′-CCATCCAATCGGTAGTAGCG-3′; GAPDH forward, 5′-GCAAATTCCATGGCACCGT-3′; and GAPDH reverse, 5′-TCGCCCCACTTGATTTTGGAGG-3′.

Clinical analyses

PTX3 determinations in GSE1561 (23) were derived from the ROCK Breast Cancer Functional Genomics database (62). PTX3 expression from breast cancer data sets in GSE1456 (24), TCGA (9), UNC337 (25), and GSE7904 (26) was derived from retrieved raw data of the original studies, which were $\log_2$-transformed and normalized at the gene level using the original normalization provided by the respective authors or using the frozen robust multiarray analysis algorithm. For survival analysis, median-centered log ratios from UNC337 were partitioned into groups of high, medium, or low PTX3 expression by comparing the median of all samples. Survival analysis was performed using Kaplan-Meier estimates using the log-rank test and the proportional hazard model to compare survival curves. For biospecimen analysis (in Fig. 2G), total RNA was extracted from cancer cell–enriched (50 to 80% tumor) macrodissected tumors using RNeasy (Qiagen) under approved Curie Institute institutional review board (IRB) protocols. Normal control tissue originated from normal tumor margins.

CCLE-derived PTX3 coexpressed genes

The expression of *PTX3* and its 19 closest coexpressed genes were determined on the indicated BCC lines using CCLE. CCLE provides public access to genomic data of multiple cancer cell lines available for analysis and visualization at www.broadinstitute.org/ccle.

Patient-derived cancer xenografts

PDX models of breast cancer were established at the Curie Institute (Paris, France), as previously published (63) under approved IRB and Institutional Animal Care and Use Committee protocols. Subtyping of TNBC PDX models was done on the basis of the published signature of Lehmann *et al.* (27) and Chen *et al.* (64).

Tumorsphere assays

Sphere-forming abilities of BCCs were conducted as previously described (29). Briefly, BCCs were seeded at 1000 cells per well in ultralow-attachment six-well plates for 5 days. Suspensions were then flushed, and >70-μm colonies were counted under a microscope. For secondary and tertiary sphere–forming activities, the primary or secondary spheres, respectively, were dissociated with Trypsin, counted, and reseeded at a density of 1000 cells per well for another 5 days.

FACS analyses

Cell lines were suspended, labeled with FITC-conjugated antibody against CD44 and PE-conjugated antibody against CD24, and processed for FACS analyses as is standard. For ALDH assays, cells were suspended in ALDEFLUOR assay buffer (STEMCELL) with ALDH1 substrate for 1 hour at 37°C and analyzed using the FITC channel. The ALDH inhibitor DEAB served as a negative control for specific ALDEFLUOR staining. FACS was conducted using the FACSCanto System (BD Biosciences).

Sulforhodamine B assay

Cell viability was assessed using sulforhodamine B (SRB) assay as previously described (65). Briefly, adherent cells were fixed with trichloroacetic acid for 1 hour at 4°C and then rinsed and stained with SRB in 1% acetic acid for at least 30 min at room temperature. Cells were then washed and allowed to dry, and solubilized SRB was measured at 510 nm.

Statistical analysis

All experiments were repeated two or three times. Results were expressed as means ± SEM. Data were analyzed using a two-sided Student's *t* test or one-way ANOVA after confirming their normal distribution. The log-rank test was used to analyze data in survival experiments. $P < 0.05$ was considered statistically significant.

Supplementary Material

Refer to Web version on PubMed Central for supplementary material.

Acknowledgments

We thank J. Hutti (AbbVie Inc.) for advice, T. Waldman (Georgetown University) and R. Weinberg (Massachusetts Institute of Technology) for providing plasmids and cells, and J. Brugge (Harvard University Medical School) for providing MCF10A cells.

Funding: We acknowledge support from the Howard Hughes Medical Institute International Student Research Fellowship (to W.H.); the American Cancer Society Postdoctoral Fellowship (to B.G.C.); NIH grants R35CA197684 (to A.S.B.), RO1-CA148761 (to C.P.), and CA177910 (to A.T.); National Cancer Institute Breast SPORE grant P50-CA58223-09A1 (to C.P.); the Sidney Kimmel Foundation (to A.E.K.); the Komen Foundation for the Cure (to A.E.K.); and the Department of Defense Breast Cancer Research Program (to A.E.K.).

References

1. Valentin MD, da Silva SD, Privat M, Alaoui-Jamali M, Bignon Y-J. Molecular insights on basal-like breast cancer. Breast Cancer Res. Treat. 2012; 134:21–30. [PubMed: 22234518]
2. Bauer KR, Brown M, Cress RD, Parise CA, Caggiano V. Descriptive analysis of estrogen receptor (ER)-negative, progesterone receptor (PR)-negative, and HER2-negative invasive breast cancer, the so-called triple-negative phenotype: A population-based study from the California cancer registry. Cancer. 2007; 109:1721–1728. [PubMed: 17387718]
3. Morris GJ, Naidu S, Topham AK, Guiles F, Xu Y, McCue P, Schwartz GF, Park PK, Rosenberg AL, Brill K, Mitchell EP. Differences in breast carcinoma characteristics in newly diagnosed African-American and Caucasian patients: A single-institution compilation compared with the National Cancer Institute's Surveillance, Epidemiology, and End Results database. Cancer. 2007; 110:876–884. [PubMed: 17620276]
4. Criscitiello C, Azim HA Jr, Schouten PC, Linn SC, Sotiriou C. Understanding the biology of triple-negative breast cancer. Ann. Oncol. 2012; 23(Suppl. 6):vi13–vi18. [PubMed: 23012296]
5. Guiu S, Michiels S, André F, Cortes J, Denkert C, Di Leo A, Hennessy BT, Sorlie T, Sotiriou C, Turner N, de Vijver MV, Viale G, Loi S, Reis-Filho JS. Molecular subclasses of breast cancer: How do we define them? The IMPAKT 2012 working group statement. Ann. Oncol. 2012:2997–3006.
6. Nielsen TO, Hsu FD, Jensen K, Cheang M, Karaca G, Hu Z, Hernandez-Boussard T, Livasy C, Cowan D, Dressler L, Akslen LA, Ragaz J, Gown AM, Blake Gilks C, van de Rijn M, Perou CM. Immunohistochemical and clinical characterization of the basal-like subtype of invasive breast carcinoma. Clin. Cancer Res. 2004; 10:5367–5374. [PubMed: 15328174]
7. Carey LA, Dees EC, Sawyer L, Gatti L, Moore DT, Collichio F, Ollila DW, Sartor CI, Graham ML, Perou CM. The triple negative paradox: Primary tumor chemosensitivity of breast cancer subtypes. Clin. Cancer Res. 2007; 13:2329–2334. [PubMed: 17438091]

8. Liedtke C, Mazouni C, Hess KR, André F, Tordai A, Mejia JA, Symmans WF, Gonzalez-Angulo AM, Hennessy B, Green M, Cristofanilli M, Hortobagyi GN, Pusztai L. Response to neoadjuvant therapy and long-term survival in patients with triple-negative breast cancer. J Clin. Oncol. 2008; 26:1275–1281. [PubMed: 18250347]
9. Cancer Genome Atlas Network. Comprehensive molecular portraits of human breast tumours. Nature. 2012; 490:61–70. [PubMed: 23000897]
10. Creighton CJ. Widespread molecular patterns associated with drug sensitivity in breast cancer cell lines, with implications for human tumors. PLOS ONE. 2013; 8:e71158. [PubMed: 24386073]
11. Klempner SJ, Myers AP, Cantley LC. What a tangled web we weave: Emerging resistance mechanisms to inhibition of the phosphoinositide 3-kinase pathway. Cancer Discov. 2013; 3:1345–1354. [PubMed: 24265156]
12. Thorpe LM, Yuzugullu H, Zhao JJ. PI3K in cancer: Divergent roles of isoforms, modes of activation and therapeutic targeting. Nat. Rev. Cancer. 2015; 15:7–24. [PubMed: 25533673]
13. Tothill RW, Tinker AV, George J, Brown R, Fox SB, Lade S, Johnson DS, Trivett MK, Etemadmoghadam D, Locandro B, Traficante N, Fereday S, Hung JA, Chiew Y-E, Haviv I, Gertig D, deFazio A, Bowtell DDL. Australian Ovarian Cancer Study Group. Novel molecular subtypes of serous and endometrioid ovarian cancer linked to clinical outcome. Clin. Cancer Res. 2008; 14:5198–5208. [PubMed: 18698038]
14. Wei Huang D, Sherman BT, Lempicki RA. Systematic and integrative analysis of large gene lists using DAVID bioinformatics resources. Nat. Protoc. 2009; 4:44–57. [PubMed: 19131956]
15. Valentino S, Gentile S, Inforzato A, Bottazzi B, Garlanda C. The long pentraxin PTX3: A paradigm for humoral pattern recognition molecules. Ann. N. Y. Acad. Sci. 2013; 1285:1–14. [PubMed: 23527487]
16. Jaillon S, Bonavita E, Gentile S, Rubino M, Laface I, Garlanda C, Mantovani A. The long pentraxin PTX3 as a key component of humoral innate immunity and a candidate diagnostic for inflammatory diseases. Int. Arch. Allergy Immunol. 2014; 165:165–178. [PubMed: 25531094]
17. Daigo K, Mantovani A, Bottazzi B. The yin-yang of long pentraxin PTX3 in inflammation and immunity. Immunol. Lett. 2014; 161:38–43. [PubMed: 24792672]
18. Salustri A, Garlanda C, Hirsch E, De Acetis M, Maccagno A, Bottazzi B, Doni A, Bastone A, Mantovani G, Beck Peccoz P, Salvatori G, Mahoney DJ, Day AJ, Siracusa G, Romani L, Mantovani A. PTX3 plays a key role in the organization of the cumulus oophorus extracellular matrix and in in vivo fertilization. Development. 2004; 131:1577–1586. [PubMed: 14998931]
19. Scarchilli L, Camaioni A, Bottazzi B, Negri V, Doni A, Deban L, Bastone A, Salvatori G, Mantovani A, Siracusa G, Salustri A. PTX3 interacts with inter-α-trypsin inhibitor: Implications for hyaluronan organization and cumulus oophorus expansion. J Biol. Chem. 2007; 282:30161–30170. [PubMed: 17675295]
20. Doni A, Musso T, Morone D, Bastone A, Zambelli V, Sironi M, Castagnoli C, Cambieri I, Stravalaci M, Pasqualini F, Laface I, Valentino S, Tartari S, Ponzetta A, Maina V, Barbieri SS, Tremoli E, Catapano AL, Norata GD, Bottazzi B, Garlanda C, Mantovani A. An acidic microenvironment sets the humoral pattern recognition molecule PTX3 in a tissue repair mode. J Exp. Med. 2015; 212:905–925. [PubMed: 25964372]
21. Bottazzi B, Inforzato A, Messa M, Barbagallo M, Magrini E, Garlanda C, Mantovan A. The pentraxins PTX3 and SAP in innate immunity, regulation of inflammation and tissue remodelling. J Hepatol. 2016; 64:1416–1427. [PubMed: 26921689]
22. Bai D, Ueno L, Vogt PK. Akt-mediated regulation of NFκB and the essentialness of NFκB for the oncogenicity of PI3K and Akt. Int. J. Cancer. 2009; 125:2863–2870. [PubMed: 19609947]
23. Farmer P, Bonnefoi H, Becette V, Tubiana-Hulin M, Fumoleau P, Larsimont D, MacGrogan G, Bergh J, Cameron D, Goldstein D, Duss S, Nicoulaz A-L, Brisken C, Fiche M, Delorenzi M, Iggo R. Identification of molecular apocrine breast tumours by microarray analysis. Oncogene. 2005; 24:4660–4671. [PubMed: 15897907]
24. Pawitan Y, Bjöhle J, Amler L, Borg A-L, Egyhazi S, Hall P, Han X, Holmberg L, Huang F, Klaar S, Liu ET, Miller L, Nordgren H, Ploner A, Sandelin K, Shaw PM, Smeds J, Skoog L, Wedrén S, Bergh J. Gene expression profiling spares early breast cancer patients from adjuvant therapy:

Derived and validated in two population-based cohorts. Breast Cancer Res. 2005; 7:R953–R964. [PubMed: 16280042]

25. Prat A, Parker JS, Karginova O, Fan C, Livasy C, Herschkowitz JI, He X, Perou CM. Phenotypic and molecular characterization of the claudin-low intrinsic subtype of breast cancer. Breast Cancer Res. 2010; 12:R68. [PubMed: 20813035]
26. Richardson AL, Wang ZC, De Nicolo A, Lu X, Brown M, Miron A, Liao X, Dirk Iglehart J, Livingston DM, Ganesan S. X chromosomal abnormalities in basal-like human breast cancer. Cancer Cell. 2006; 9:121–132. [PubMed: 16473279]
27. Lehmann BD, Bauer JA, Chen X, Sanders ME, Chakravarthy AB, Shyr Y, Pietenpol JA. Identification of human triple-negative breast cancer subtypes and preclinical models for selection of targeted therapies. J Clin. Invest. 2011; 121:2750–2767. [PubMed: 21633166]
28. Taube JH, Herschkowitz JI, Komurov K, Zhou AY, Gupta S, Yang J, Hartwell K, Onder TT, Gupta PB, Evans KW, Hollier BG, Ram PT, Lander ES, Rosen JM, Weinberg RA, Mani SA. Core epithelial-to-mesenchymal transition interactome gene-expression signature is associated with claudin-low and metaplastic breast cancer subtypes. Proc. Natl. Acad. Sci. U.S.A. 2010; 107:15449–15454. [PubMed: 20713713]
29. El-Haibi CP, Bell GW, Zhang J, Collmann AY, Wood D, Scherber CM, Csizmadia E, Mariani O, Zhu C, Campagne A, Toner M, Bhatia SN, Irimia D, Vincent-Salomon A, Karnoub AE. Critical role for lysyl oxidase in mesenchymal stem cell-driven breast cancer malignancy. Proc. Natl. Acad. Sci. U.S.A. 2012; 109:17460–17465. [PubMed: 23033492]
30. Moreno-Bueno G, Salvador F, Martín A, Floristán A, Cuevas EP, Santos V, Montes A, Morales S, Angeles Castilla M, Rojo-Sebastián A, Martínez A, Hardisson D, Csiszar K, Portillo F, Peinado H, Palacios J, Cano A. Lysyl oxidase-like 2 (LOXL2), a new regulator of cell polarity required for metastatic dissemination of basal-like breast carcinomas. EMBO Mol. Med. 2011; 3:528–544. [PubMed: 21732535]
31. Gupta PB, Onder TT, Jiang G, Tao K, Kuperwasser C, Weinberg RA, Lander ES. Identification of selective inhibitors of cancer stem cells by high-throughput screening. Cell. 2009; 138:645–659. [PubMed: 19682730]
32. Asiedu MK, Beauchamp-Perez FD, Ingle JN, Behrens MD, Radisky DC, Knutson KL. AXL induces epithelial-to-mesenchymal transition and regulates the function of breast cancer stem cells. Oncogene. 2014; 33:1316–1324. [PubMed: 23474758]
33. Wang C-A, Harrell JC, Iwanaga R, Jedlicka P, Ford HL. Vascular endothelial growth factor C promotes breast cancer progression via a novel antioxidant mechanism that involves regulation of superoxide dismutase 3. Breast Cancer Res. 2014; 16:462. [PubMed: 25358638]
34. Jang MH, Kim HJ, Kim EJ, Chung YR, Park SY. Expression of epithelial-mesenchymal transition-related markers in triple-negative breast cancer: ZEB1 as a potential biomarker for poor clinical outcome. Hum. Pathol. 2015; 46:1267–1274. [PubMed: 26170011]
35. Ginestier C, Hur MH, Charafe-Jauffret E, Monville F, Dutcher J, Brown M, Jacquemier J, Viens P, Kleer CG, Liu S, Schott A, Hayes D, Birnbaum D, Wicha MS, Dontu G. ALDH1 is a marker of normal and malignant human mammary stem cells and a predictor of poor clinical outcome. Cell Stem Cell. 2007; 1:555–567. [PubMed: 18371393]
36. Hutti JE, Pfefferle AD, Russell SC, Sircar M, Perou CM, Baldwin AS. Oncogenic PI3K mutations lead to NF-κB–Dependent cytokine expression following growth factor deprivation. Cancer Res. 2012; 72:3260–3269. [PubMed: 22552288]
37. Dubrovska A, Kim S, Salamone RJ, Walker JR, Maira S-M, García-Echeverría C, Schultz PG, Reddy VA. The role of PTEN/Akt/PI3K signaling in the maintenance and viability of prostate cancer stem-like cell populations. Proc. Natl. Acad. Sci. U.S.A. 2009; 106:268–273. [PubMed: 19116269]
38. Korkaya H, Paulson A, Charafe-Jauffret E, Ginestier C, Brown M, Dutcher J, Clouthier SG, Wicha MS. Regulation of mammary stem/progenitor cells by PTEN/Akt/β-catenin signaling. PLOS Biol. 2009; 7:e1000121. [PubMed: 19492080]
39. Park SY, Lee HE, Li H, Shipitsin M, Gelman R, Polyak K. Heterogeneity for stem cell-related markers according to tumor subtype and histologic stage in breast cancer. Clin. Cancer Res. 2010; 16:876–887. [PubMed: 20103682]

40. Yamamoto M, Taguchi Y, Ito-Kureha T, Semba K, Yamaguchi N, Inoue J-i. NF-κB non-cell-autonomously regulates cancer stem cell populations in the basal-like breast cancer subtype. Nat. Commun. 2013; 4:2299. [PubMed: 23934482]
41. Kendellen MF, Bradford JW, Lawrence CL, Clark KS, Baldwin AS. Canonical and non-canonical NF-κB signaling promotes breast cancer tumor-initiating cells. Oncogene. 2014; 33:1297–1305. [PubMed: 23474754]
42. Kolev VN, Wright QG, Vidal CM, Ring JE, Shapiro IM, Ricono J, Weaver DT, Padval MV, Pachter JA, Xu Q. PI3K/mTOR dual inhibitor VS-5584 preferentially targets cancer stem cells. Cancer Res. 2015; 75:446–455. [PubMed: 25432176]
43. Brooks MD, Burness ML, Wicha MS. Therapeutic implications of cellular heterogeneity and plasticity in breast cancer. Cell Stem Cell. 2015; 17:260–271. [PubMed: 26340526]
44. Diamandis EP, Goodglick L, Planque C, Thornquist MD. Pentraxin-3 is a novel biomarker of lung carcinoma. Clin. Cancer Res. 2011; 17:2395–2399. [PubMed: 21257721]
45. Infante M, Allavena P, Garlanda C, Nebuloni M, Morenghi E, Rahal D, Roncalli M, Cavuto S, Pesce S, Monari M, Valaperta S, Montanelli A, Solomon D, Bottoni E, Errico V, Voulaz E, Bossi M, Chiesa G, Passera E, Mantovani A, Alloisio M. Prognostic and diagnostic potential of local and circulating levels of pentraxin 3 in lung cancer patients. Int. J. Cancer. 2016; 138:983–991. [PubMed: 26348770]
46. Stallone G, Cormio L, Netti GS, Infante B, Selvaggio O, Fino GD, Ranieri E, Bruno F, Prattichizzo C, Sanguedolce F, Tortorella S, Bufo P, Grandaliano G, Carrieri G. Pentraxin 3: A novel biomarker for predicting progression from prostatic inflammation to prostate cancer. Cancer Res. 2014; 74:4230–4238. [PubMed: 24950910]
47. Carmo RF, Aroucha D, Vasconcelos LR, Pereira LM, Moura P, Cavalcanti MS. Genetic variation in *PTX3* and plasma levels associated with hepatocellular carcinoma in patients with HCV. J Viral Hepat. 2016; 23:116–122. [PubMed: 26400151]
48. Kondo S, Ueno H, Hosoi H, Hashimoto J, Morizane C, Koizumi F, Tamura K, Okusaka T. Clinical impact of pentraxin family expression on prognosis of pancreatic carcinoma. Br. J. Cancer. 2013; 109:739–746. [PubMed: 23828517]
49. Barbui T, Carobbio A, Finazzi G, Vannucchi AM, Barosi G, Antonioli E, Guglielmelli P, Pancrazzi A, Salmoiraghi S, Zilio P, Ottomano C, Marchioli R, Cuccovillo I, Bottazzi B, Mantovani A, Rambaldi A. AGIMM and IIC Investigators, Inflammation and thrombosis in essential thrombocythemia and polycythemia vera: Different role of C-reactive protein and pentraxin 3. Haematologica. 2011; 96:315–318. [PubMed: 21173097]
50. Scimeca M, Antonacci C, Colombo D, Bonfiglio R, Buonomo OC, Bonanno E. Emerging prognostic markers related to mesenchymal characteristics of poorly differentiated breast cancers. Tumor Biol. 2016; 37:5427–5435.
51. Chi J-Y, Hsiao Y-W, Li C-F, Lo Y-C, Lin Z-Y, Hong J-Y, Liu Y-M, Han X, Wang S-M, Chen B-K, Tsai KK, Wang J-M. Targeting chemotherapy-induced PTX3 in tumor stroma to prevent the progression of drug-resistant cancers. Oncotarget. 2015; 6:23987–24001. [PubMed: 26124179]
52. Rusnati M, Camozzi M, Moroni E, Bottazzi B, Peri G, Indraccolo S, Amadori A, Mantovani A, Presta M. Selective recognition of fibroblast growth factor-2 by the long pentraxin PTX3 inhibits angiogenesis. Blood. 2004; 104:92–99. [PubMed: 15031207]
53. Leali D, Alessi P, Coltrini D, Ronca R, Corsini M, Nardo G, Indraccolo S, Presta M. Long pentraxin-3 inhibits FGF8b-dependent angiogenesis and growth of steroid hormone–regulated tumors. Mol. Cancer Ther. 2011; 10:1600–1610. [PubMed: 21764903]
54. Ronca R, Di Salle E, Giacomini A, Leali D, Alessi P, Coltrini D, Ravelli C, Matarazzo S, Ribatti D, Vermi W, Presta M. Long pentraxin-3 inhibits epithelial–mesenchymal transition in melanoma cells. Mol. Cancer Ther. 2013; 12:2760–2771. [PubMed: 24130051]
55. Ronca R, Giacomini A, Di Salle E, Coltrini D, Pagano K, Ragona L, Matarazzo S, Rezzola S, Maiolo D, Torella R, Moroni E, Mazzieri R, Escobar G, Mor M, Colombo G, Presta M. Long-pentraxin 3 derivative as a small-molecule FGF trap for cancer therapy. Cancer Cell. 2015; 28:225–239. [PubMed: 26267536]
56. Bonavita E, Gentile S, Rubino M, Maina V, Papait R, Kunderfranco P, Greco C, Feruglio F, Molgora M, Laface I, Tartari S, Doni A, Pasqualini F, Barbati E, Basso G, Galdiero MR, Nebuloni

M, Roncalli M, Colombo P, Laghi L, Lambris JD, Jaillon S, Garlanda C, Mantovani A. PTX3 is an extrinsic oncosuppressor regulating complement-dependent inflammation in cancer. Cell. 2015; 160:700–714. [PubMed: 25679762]

57. Wang J-X, He Y-L, Zhu S-T, Yang S, Zhang S-T. Aberrant methylation of the 3q25 tumor suppressor gene *PTX3* in human esophageal squamous cell carcinoma. World J. Gastroenterol. 2011; 17:4225–4230. [PubMed: 22072855]
58. Tsuji S, Midorikawa Y, Seki M, Takayama T, Sugiyama Y. Network-based analysis for identification of candidate genes for colorectal cancer progression. Biochem. Biophys. Res. Commun. 2016; 476:534–540. [PubMed: 27255996]
59. Acerbi I, Cassereau L, Dean I, Shi Q, Au A, Park C, Chen YY, Liphardt J, Hwang ES, Weaver VM. Human breast cancer invasion and aggression correlates with ECM stiffening and immune cell infiltration. Integr. Biol. 2015; 7:1120–1134.
60. Weigman VJ, Chao H-H, Shabalin AA, He X, Parker JS, Nordgard SH, Grushko T, Huo D, Nwachukwu C, Nobel A, Kristensen VN, Børresen-Dale A-L, Olopade OI, Perou CM. Basal-like breast cancer DNA copy number losses identify genes involved in genomic instability, response to therapy, and patient survival. Breast Cancer Res. Treat. 2012; 133:865–880. [PubMed: 22048815]
61. Ziegelbauer K, Gantner F, Lukacs NW, Berlin A, Fuchikami K, Niki T, Sakai K, Inbe H, Takeshita K, Ishimori M, Komura H, Murata T, Lowinger T, Bacon KB. A selective novel low-molecular-weight inhibitor of IκB kinase-β (IKK-β) prevents pulmonary inflammation and shows broad anti-inflammatory activity. Br. J. Pharmacol. 2005; 145:178–192. [PubMed: 15753951]
62. Ur-Rehman S, Gao Q, Mitsopoulos C, Zvelebil M. ROCK: A resource for integrative breast cancer data analysis. Breast Cancer Res. Treat. 2013; 139:907–921. [PubMed: 23756628]
63. Marangoni E, Vincent-Salomon A, Auger N, Degeorges A, Assayag F, de Cremoux P, de Plater L, Guyader C, De Pinieux G, Judde J-G, Rebucci M, Tran-Perennou C, Sastre-Garau X, Sigal-Zafrani B, Delattre O, Diéras V, Poupon M-F. A new model of patient tumor-derived breast cancer xenografts for preclinical assays. Clin. Cancer Res. 2007; 13:3989–3998. [PubMed: 17606733]
64. Chen X, Li J, Gray WH, Lehmann BD, Bauer JA, Shyr Y, Pietenpol JA. TNBCtype: A subtyping tool for triple-negative breast cancer. Cancer Inf. 2012; 11:147–156.
65. Brown KK, Montaser-Kouhsari L, Beck AH, Toker A. MERIT40 is an Akt substrate that promotes resolution of DNA damage induced by chemotherapy. Cell Rep. 2015; 11:1358–1366. [PubMed: 26027929]
66. Lu X, Lu X, Wang ZC, Iglehart JD, Zhang X, Richardson AL. Predicting features of breast cancer with gene expression patterns. Breast Cancer Res. Treat. 2008; 108:191–201. [PubMed: 18297396]

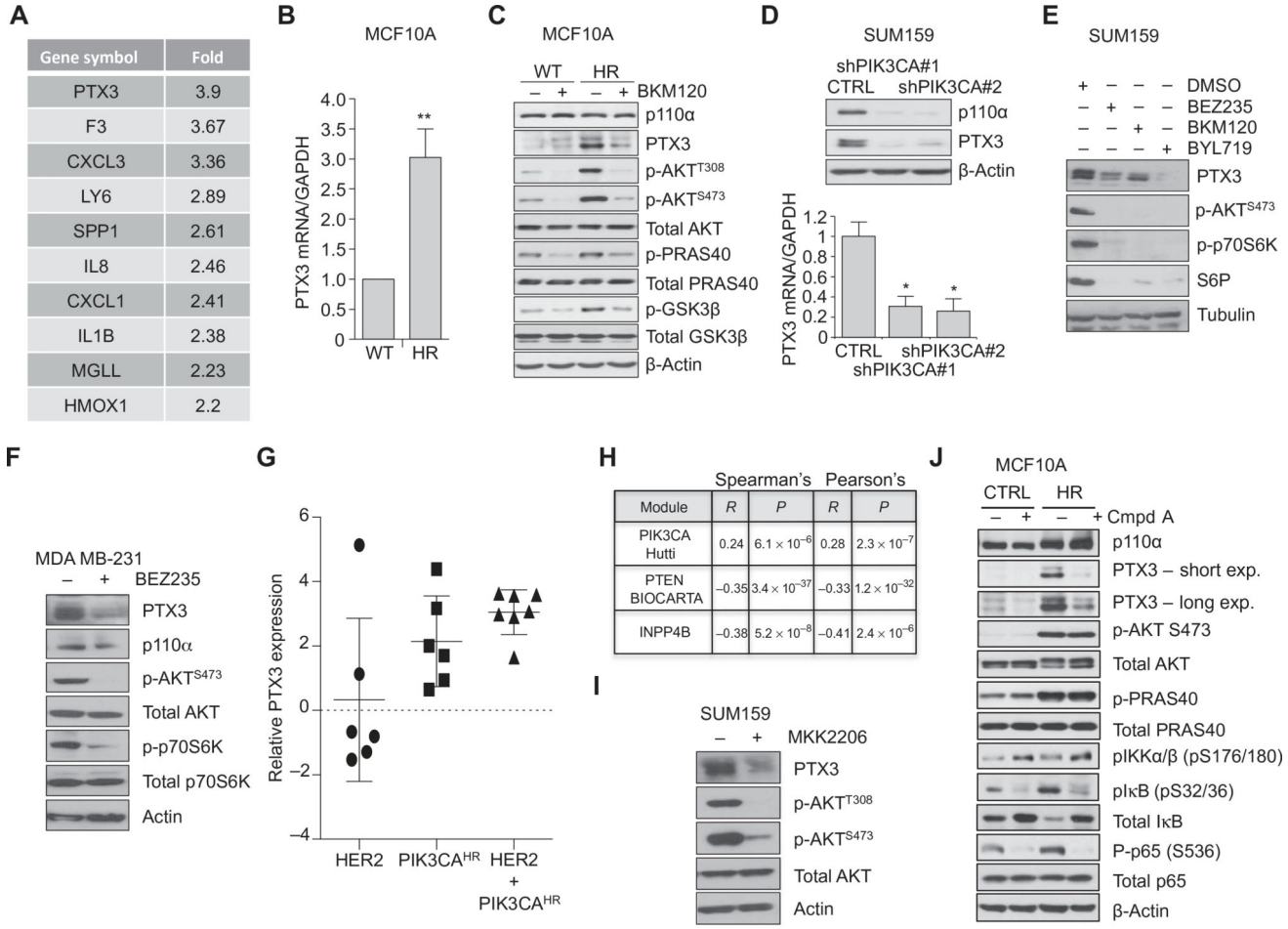

Fig. 1. PI3K activation triggers PTX3 expression in BLBC cells

(**A**) Fold induction of the top 10 genes up-regulated by PIK3CA^{H1047R} (HR) expression in MCF10A cells relative to wild-type (WT) PIK3CA expression. (**B**) Quantitative reverse transcription polymerase chain reaction (qRT-PCR) measurements of *PTX3* mRNA abundance in MCF10A cells stably expressing WT (13) or HR. Data are means ± SEM of n = 3 independent experiments, each performed in triplicate. GAPDH, glyceraldehyde-3-phosphate dehydrogenase. (**C**) Representative Western blot analysis of MCF10A cells stably expressing WT or HR treated with BKM120 (1 μM for 24 hours) (+) or vehicle control (−) and deprived of epidermal growth factor (EGF) and insulin (n > 3). (**D**) Top: Representative Western blot of SUM159 cells stably expressing control (CTRL) or *PIK3CA* shRNAs. Bottom: qRT-PCR measurements of *PTX3* mRNA normalized to *GAPDH* in the indicated SUM159 variants. Data are means ± SEM of n = 3 independent experiments, each performed in triplicate. (**E**) Representative Western blot analysis of SUM159 cells treated with vehicle (−), BEZ235 (5 μM), BKM120 (1 μM), or BYL719 (1 μM) for 24 hours (n > 3). (**F**) Representative Western blot analysis of MDA-MB-231 cells treated with vehicle (−) or with BEZ235 (5 μM) for 24 hours (n > 3). (**G**) *PTX3* transcript abundance derived from microarrays of mouse tumors (GSE41118) driven by HER2 (n = 6), HR (n = 6), or HER2 + HR (n = 7). (**H**) Spearman's and Pearson's correlation analyses of *PTX3* expression with that of activated *PIK3CA* gene signature derived from Hutti *et al.* (36), *PTEN* BIOCARTA

pathway, and *INPP4B* gene in the UNC337, The Cancer Genome Atlas (TCGA), and in GSE5460 (66) databases, respectively. (**I**) Representative Western blot analysis of SUM159 cells treated with vehicle (−) or MK2206 (1 μM) for 24 hours ($n > 3$). (**J**) Representative Western blot analysis of control or HR MCF10A cells treated with compound A (Cmpd A; 5 μM) for 24 hours ($n > 3$). *$P < 0.05$ and **$P < 0.01$, by unpaired t test. Exp., exposure.

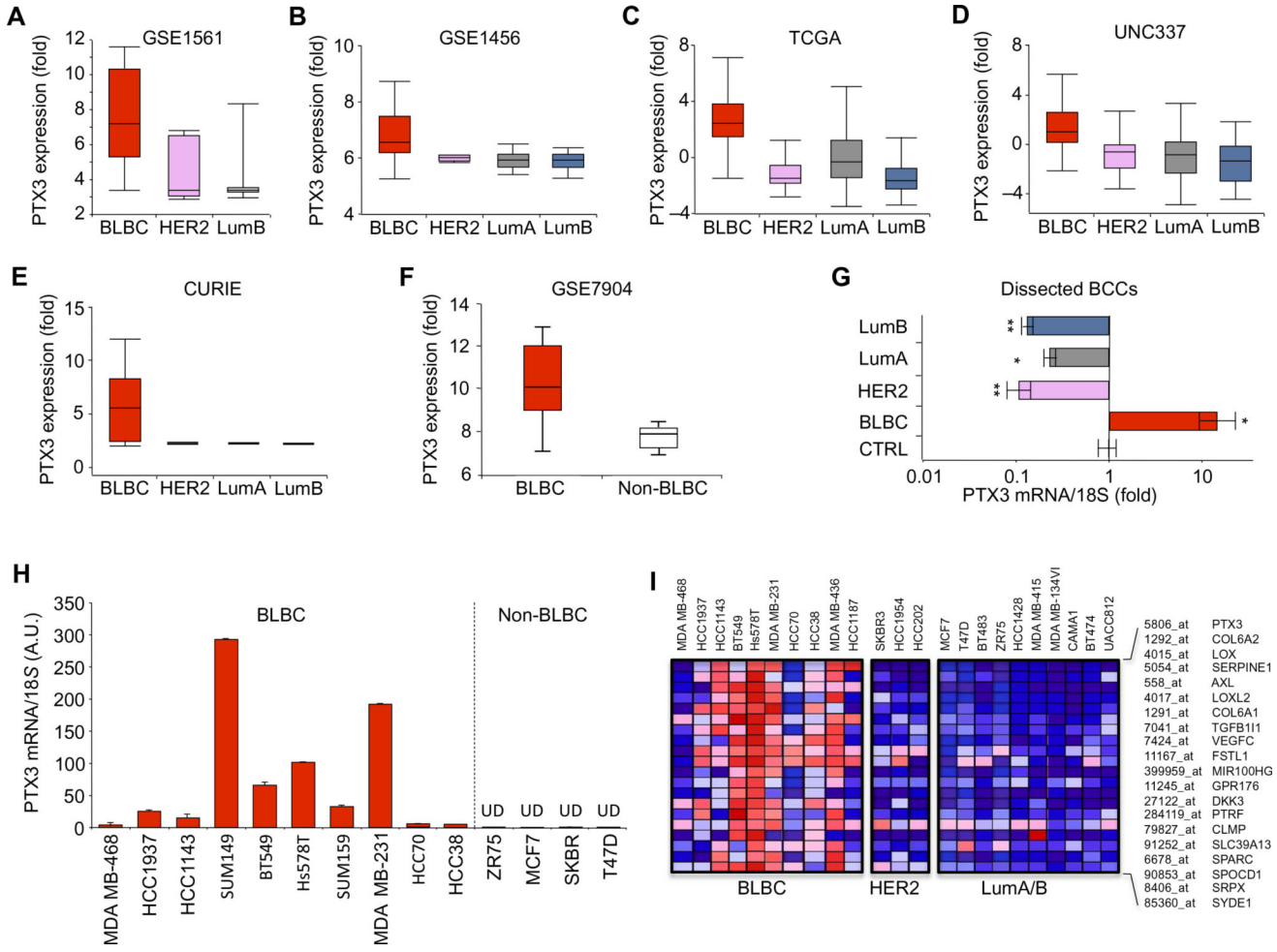

Fig. 2. PTX3 expression is specifically associated with BLBCs

(**A**) *PTX3* expression (probe 206157_at) in GSE1561 analyzed using significance analysis of microarrays (SAMs) in ROCK Breast Cancer Functional Genomics database: BLBC (n = 15), HER2 (n = 8), and LumB (n = 23); FDR, 0%. (**B**) *PTX3* expression (probe 206157_at) in GSE1456 analyzed by SAMs: BLBC (n = 25), HER2 (n = 15), LumA (n = 39), LumB (n = 23); FDR, 0%. (**C**) Analysis of variance (ANOVA) box plot analyses for *PTX3* (probe 206157_at) in TCGA; $P = 5.63 \times 10^{-50}$. (**D**) ANOVA box plot analyses for *PTX3* (probe 206157_at) in UNC337; $P = 2.97 \times 10^{-32}$. (**E**) ANOVA box plot analysis of *PTX3* (probe 206157_at) in breast cancer samples collected at the Curie Institute: BLBC (n = 78),HER2 (n = 31), LumA (n = 28), and LumB (n = 32); $P = 4.89 \times 10^{-25}$. (**F**) ANOVA box plot analysis of *PTX3* (probe 206157_at) in GSE7904; BLBC (n = 18) and non-BLBC (n = 21); $P = 1.723 \times 10^{-9}$. (**G**) qRT-PCR analysis of *PTX3* expression in RNA from dissected BCCs lifted off slides of the indicated tumor samples: Control (n = 5), BLBC (n = 16), HER2 (n = 13), LumA (n = 25), LumB (n = 22). *$P < 0.05$ and **$P < 0.01$, by unpaired t test. (**H**) qRT-PCR measurements (means ± SEM of $n > 3$) of *PTX3* mRNA abundance in the indicated BCC lines. Values were normalized to that of 18*S* and are displayed as arbitrary units (A.U.). (**I**) *PTX3* and 19 most closely associated genes across all the cancer cells represented in the Broad Institute CCLE (called here “PTX3 gene signature”) were profiled in the

indicated BCC lines, grouped according to breast tumor subtype. Red and blue indicate increased and diminished expression of *PTX3*, respectively.

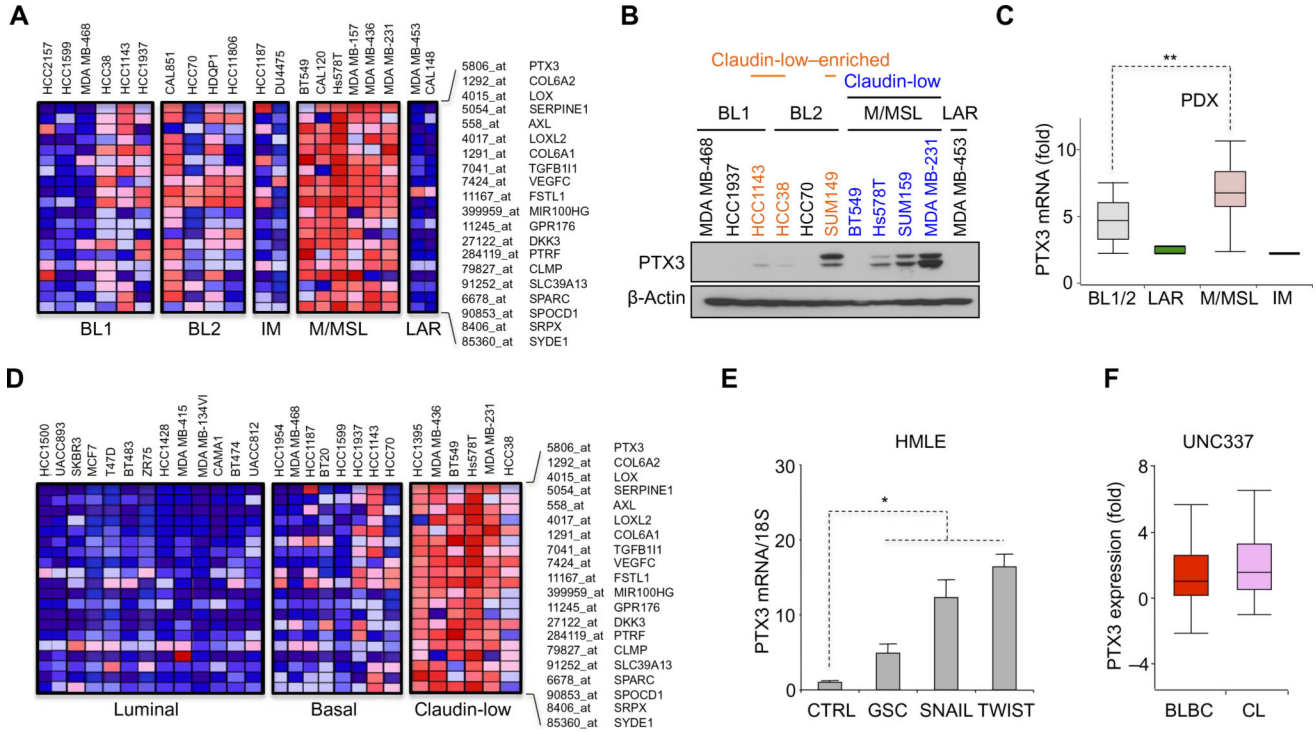

Fig. 3. PTX3 is particularly enriched in M/MSL/CL BCCs

(**A**) *PTX3* gene expression signature in the indicated BLBC subclasses from Lehmann *et al.* (27). (**B**) Representative Western blot on PTX3 in the indicated BCC lines ($n > 3$). (**C**) ANOVA box plot of *PTX3* expression (NM_00282) in PDX models of indicated breast cancer subtypes. BL1/2 ($n = 13$), LAR ($n = 2$), M/MSL ($n = 11$), IM ($n = 1$); $P = 0.008$. (**D**) *PTX3* gene signature across the indicated BCC lines, grouped according to molecular classification (25). (**E**) qRT-PCR analyses of *PTX3* mRNA in HMLE cells stably expressing the transcription factors GSC, SNAIL, and TWIST, relative to that in controls. Data are means ± SEM of triplicates from ≥3 independent experiments. $*P < 0.05$ and $**P < 0.01$, by unpaired *t* test. (**F**) ANOVA box plot analyses for *PTX3* expression (probe 206157_at) in BLBC and CL subtypes from the UNC337 database; $P = 1.07 \times 10^{-4}$.

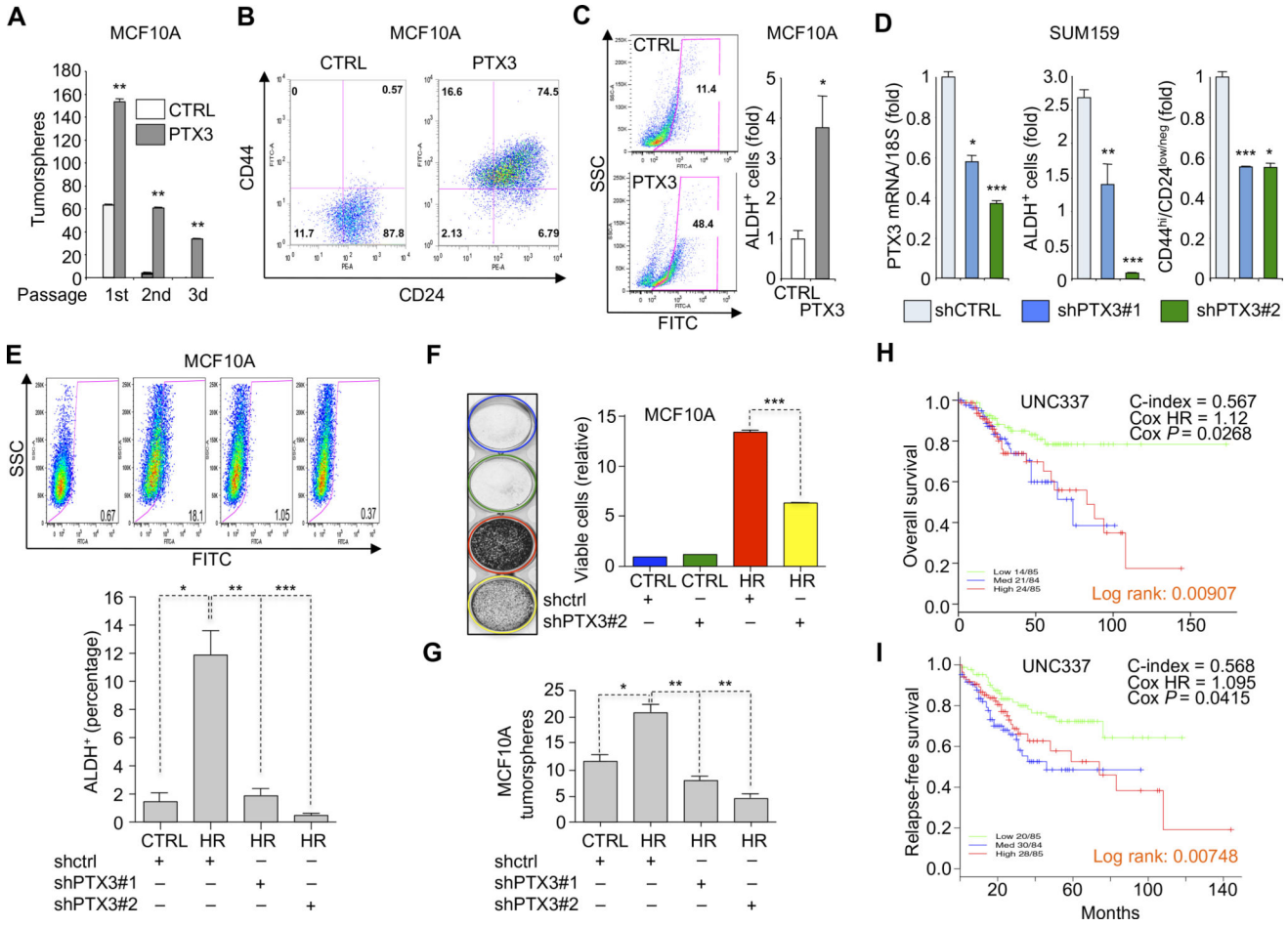

Fig. 4. PTX3 is a critical and functional effector of PI3K signaling

(**A**) Controls or PTX3-expressing MCF10A cells were plated in triplicates in low-adherence plates and scored for their ability to form tumorspheres after the indicated serial passages. Data are means ± SEM of triplicates from ≥3 independent experiments. (**B** and **C**) Controls or stable PTX3-expressing MCF10A cells were analyzed for their expression of CD44 [fluorescein isothiocyanate (FITC)] and CD24 [phycoerythrin (PE)] (B) or ALDH positivity (C) (red gate) using FACS (fluorescence-activated cell sorting). Data are representative of more than three experiments. (**D**) qRT-PCR measurements of *PTX3* mRNA abundance in SUM159 cells stably expressing control or PTX3-specific shRNA molecules. Variants expressing the indicated shRNA were analyzed for their ALDH positivity and CD44/CD24 expression using FACS. Data are means ± SEM in triplicates of more than three independent experiments. (**E**) ALDH positivity of controls or MCF10A cells harboring control shRNA (shctrl) or shPTX3 constructs in the WT or HR backgrounds. Data are means ± SEM from ≥3 experiments. (**F**) Representative images of sulforhodamine-stained, 4-day cultured MCF10A cells stably expressing HR or controls, along with shctrl or shPTX3. Viable cell count was determined colorimetrically. Data are means ± SEM of three independent biological replicates, each performed in triplicate. (**G**) Control or shPTX3-expressing MCF10A cells harboring control or HR expression vectors were plated in triplicates in low-adherence plates and scored for their ability to form tumorspheres at first passage. Data are

means ± SEM of triplicates from ≥3 independent experiments. (**H** and **I**) Kaplan-Meier analysis of overall survival (H) and relapse-free survival (I) in UNC337 estimated on patient cohorts whose breast tumors harbored low, medium, and high *PTX3* expression. (H) $P = 0.00907$ and (I) $P = 0.00748$, calculated by log-rank test. (A, C, D, E, and G) $*P < 0.05$, $**P < 0.01$, and $***P < 0.001$, by unpaired *t* test. SSC, side scatter.